

Predicting radiated emissions from cables in the RE02/RE102/DO-160/SAE J113-41 test set up, using measured current in NEC and simple TX equations.

D. A. Weston
NARTE Certified EMC Engineer

RE02Tx.rep

14-6-2004

THIS REPORT IS PART OF A RESEARCH PROGRAM AND THE CONTENT, OR ANY PART THEREOF, MAY BE REPRODUCED AS LONG AS THE SOURCE IS RECOGNIZED AS FOLLOWS:

Reproduced by permission of EMC Consulting Inc. from the report “Predicting radiated emissions from cables in the RE02/RE102/DO-160/SAE J113-42 test set up, using measured current in the NEC and simple TX equations”.

1) Introduction

It is often required to predict the radiated emissions from cables in the typical radiated emission test set up in an anechoic chamber or absorber loaded room. A set up specified by the military, space, civilian aircraft and automotive industries has the cable of 2m length at a height of 0.05m and 0.1m from the front edge of a ground plane with the measuring antenna at a distance of 1m from the Equipment Under Test (EUT)/cable. These types of measurements are notoriously inaccurate when performed in a shielded room with no absorber. This is due to the EUT exciting TEM resonances in the room and also multiple reflections within the room. Even the MIL-STD-461D/E, MIL-STD-462D room which specifies a minimum amount of damping suffers from an enhancement or reduction in the measured field due to these effects when compared to measurements made on an Open Area Test Site (OATS). Unfortunately the OATS is not suitable for this type of test due to the low specified limits on the radiated emissions compared to the ambient.

Measurements may be made in the laboratory of the current flow on the interconnection cables using a current probe, preamplifier and spectrum analyzer. The EUT is bonded to the copper or brass ground plane with the 2m long cable located above the ground plane. This cable current can then be used in either the Numerical Electromagnetic Code (NEC) or simple equations presented in reference 1 and in appendix 1 of this report, to predict the radiated emissions in the near field at a distance of 1m. If a spectrum analyzer and current probe are not available then an alternative, for an unshielded cable which is unterminated from the chassis at the far end, is the use of an oscilloscope. The oscilloscope would require a 250MHz bandwidth and a 5mV sensitivity to predict emissions and compare them to MIL-STD-461E. The voltage is measured between the unshielded cable and the ground plane at the EUT end of the cable. The voltage may be used in the NEC program directly as the value of the voltage source. When using the simple transmission line equation the current is required and this can be calculated based on the input impedance provided on page 177 of reference 1 and then used in the equations presented in appendix 1 of this report. However it must be said that the current probe or oscilloscope measurements, when made in a laboratory and not a shielded room, are often difficult due to the high level of ambient which induces current and noise voltages into the line.

2) Open circuited and short circuited cables

If the interconnection cable is shielded it is typically connected to ground at the EUT at one end and to the enclosure of auxiliary equipment, the shielded room wall or the ground plane at the other end. Even if the cable is unshielded it may have an RF connection to chassis and the ground plane through some impedance such as capacitors in a filter or a capacitor, or even a direct dc connection, between signal ground and chassis.

This impedance may be low at some frequencies and is typically complex resulting in high impedances at other frequencies.

In some cases unshielded cables are deliberately disconnected from ground, although above some frequency an RF connection exists due to parasitic capacitances and mutual inductance between the wire/PCB traces and enclosure.

For cables which are deliberately isolated from chassis (the ground plane) the prediction of radiation from a cable open circuited at one end is of interest. Here we assume that the

which is then added to the predicted field (because we know the predicted current was lower than the measured) of

$$E_{zp} = 51.29 \text{ dB}\mu\text{V/m}$$

to give us a normalized field prediction

$$\begin{aligned} E_{zpn} &= E_{zp} + \Delta \\ &= 51.29 \text{ dB}\mu\text{V/m} + 36.67 \text{ dB} \\ &= 87.96 \text{ dB}\mu\text{V/m} \end{aligned}$$

4) Radiated emission measurements in MIL-STD-461D/E shielded rooms, anechoic chambers and the damped room used for the measurements described here.

“In a typical RE02 measurement some reflections and TEM modes are set up even in a well damped room and the correlation between modeling techniques and RE02 measurements in a damped room can be as high as 12dB. For measurements made in a room with the minimum level of damping specified in MIL-STD-461D/E these errors can be higher and in a completely undamped room with a high Q the errors can be as high as +/-30dB when compared to measurements made on the OATS, against which all measurements should be compared..

The SAE J1113-41 specification for electromagnetic radiation of components on-board vehicles requires that in the 70 - 1000MHz frequency range that the maximum error caused by reflected energy from the walls and ceiling is less than 6dB. The room used for the measurements described in this report shows a correlation of 6dB between 50MHz and 1000MHz. However at 24MHz and 37MHz TEM modes are excited and the errors increase to up to 10dB when compared to the OATS measurements.

5) Open Circuit Radiated and conducted test set up and measurements

5.1 Test Procedure

Test equipment was set up as shown in figure 5.1. The signal generator used was a Marconi 2018A set to an output RF level of +10dBm. The cable was simulated by braid and this was the Belden Tin Cu shielding and bonding cable with an outside diameter of 4mm. A 50Ω series resistor was connected between the output of the signal generator and the end of the braid wire. This 50Ω resistor simulates the noise source impedance. The braid wire was raised 5cm above the surface, using styrofoam blocks, and 10cm from the edge of the ground plane. The receiving antenna stood 1m from the center of the 2m braid wire. For 1-24MHz this antenna was a 1m monopole, coupled to the ground plane. At 1 MHz and 1.2MHz an FET buffer was also added. From 37.5MHz to 250MHz both horizontal and vertical fields were measured by a log-periodic biconical antenna, however

a bowtie antenna yielded similar results for both orientations and this also consistent with a good measured correlation between the log - periodic biconical antenna and a set of “Roberts” reference dipoles . Outside of the anechoic chamber, the IFR Systems AN930 S/A was used to alternately measure the current flowing on the braid wire and the field received by the antenna. All measurements were taken in dB μ V and correction factors were applied for the Antenna Factor and the FET buffer where necessary.

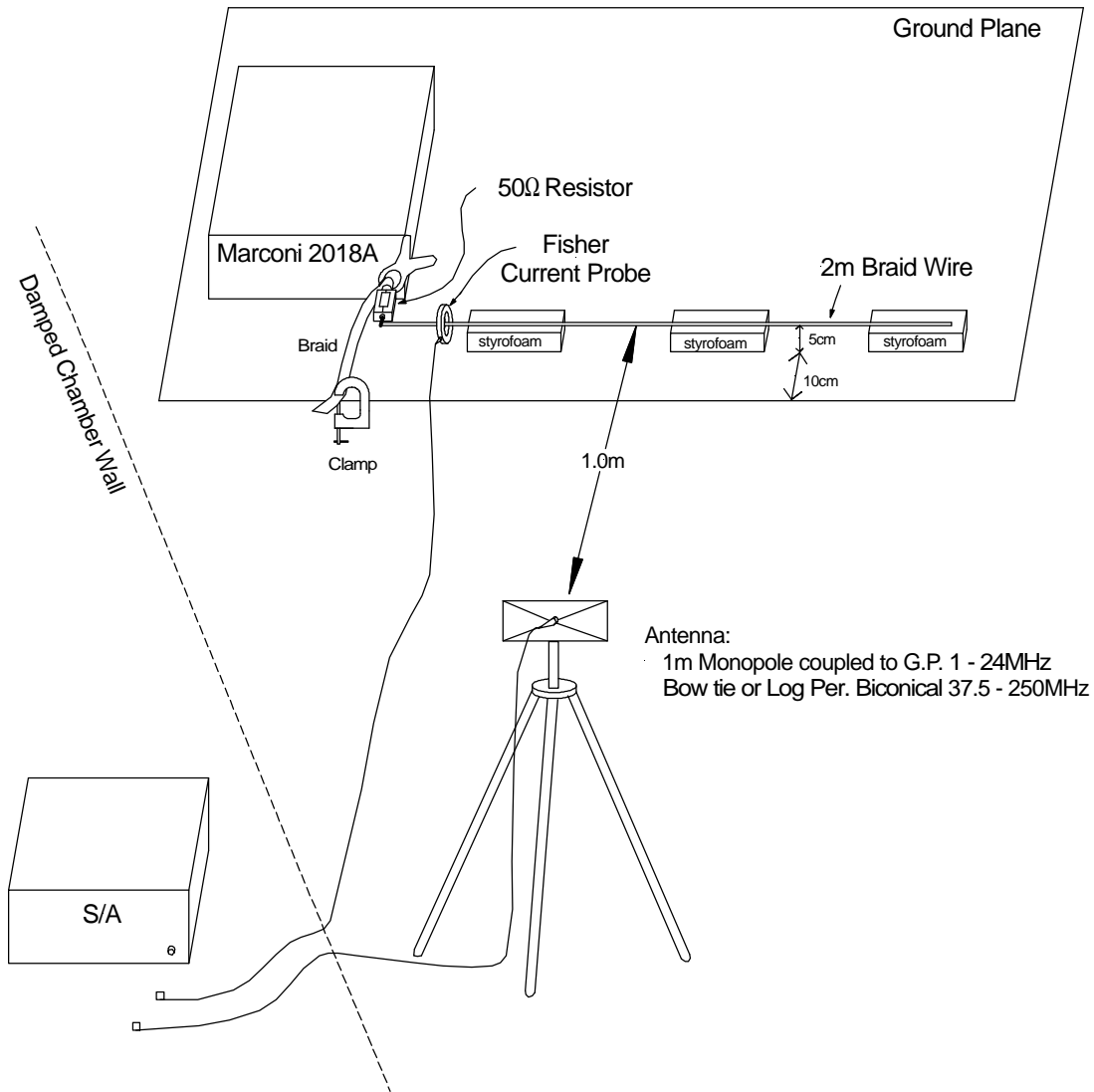


Figure 5.1. Test set up.

5.2 Test Results and Calculations

Table 1 shows the data measured from the current probe around the braid wire and the transfer impedance of the current probe. Currents were calculated in the following fashion.

$$I = V/R$$

Taking the log of both sides we get,

$$\begin{aligned} \text{Log } I &= \text{Log } (V/R) \\ &= \text{Log } V - \text{Log } R \end{aligned}$$

Multiplying both sides by 20 to arrive at dB we get,

$$20 \text{ Log } I = 20 \text{ Log } V - 20 \text{ Log } R$$

For example, at 1 MHz,

$$\begin{aligned} I \text{ (dB}\mu\text{A)} &= 53.3 \text{ dB}\mu\text{V} - 6.5 \text{ dB}\Omega \\ I &= 46.8 \text{ dB}\mu\text{A} \end{aligned}$$

Table 2 shows the measured E-field components in the vertical (Ez) and horizontal (Ey) directions. To get the total electric field components, antenna factors are added to the measured data as shown in the following example.

At 1 MHz,

$$\begin{aligned} \text{Total } E_z &= \text{Data (dB}\mu\text{V)} + \text{Antenna Factor (dB)} \\ &= 58.3 \text{ dB}\mu\text{V} + 9.3 \text{ dB} \\ &= 67.6 \text{ dB}\mu\text{V/m} \end{aligned}$$

Note that all the requirements specify the measurement of only vertically polarized fields up to 30MHz and so no Ey measurements were made until above 30MHz, after which both vertically and horizontally polarized fields were measured..

Table 1
Current Probe Measurements Taken in the Shielded Room. O/C line

Frequency (MHz)	Data (dB μ V)	Current Probe Z_t (dB Ω)	Current (dB μ A)
1	53.3	6.5	46.8
1.2	55.5	7.2	48.3
10	80.8	14.0	66.8
20	89.2	14.6	74.6
24	92.0	14.6	77.4

37.5	90.4	15.2	75.2
50	91.3	15.5	75.8
62.3	83.5	15.2	68.3
100	92.0	14.9	77.1
112.5	94.8	15.0	79.8
134.9	84.1	14.8	69.3
180.48	93.8	14.3	79.5
187.5	92.0	14.0	78.0
190	91.3	13.8	77.5
200	87.6	13.3	74.3
250	87.6	11.5	76.1

Table 2
E-Field Measurements Taken in the Damped chamber/Shielded Room O/C line

Frequency (MHz)	Antenna Vertical			Antenna Horizontal		
	Data (dB μ V)	AF (dB)	Total Ez (dB μ V/m)	Data (dB μ V)	AF (dB)	Total Ey (dB μ V/m)
1*	58.3	9.3	67.6			
1.2*	58.3	10.3	68.6			
10	34.2	33.0	67.2			
20	73.0	30.3	103.3			
24	66.4	26.0	92.4			
37.5	69.5	20.3	89.8	66.0	20.3	86.3
50	81.0	17.8	98.8	73.5	17.8	91.3
62.3	73.8	14.5	88.3	65.4	14.5	79.9
100	65.1	9.7	74.8	81.6	9.7	91.3
112.5	66.0	10.0	76.0	85.1	10.0	95.1
134.9	80.1	12.8	92.9	74.1	12.8	86.9
180.48	82.0	9.3	91.3	86.6	9.3	95.9
187.5	77.3	9.4	86.7	85.1	9.4	94.5
190	75.4	9.4	84.8	83.2	9.4	92.6
200	77.0	9.4	86.4	80.1	9.4	89.5
250	79.8	10.5	90.3	77.6	10.5	88.1

* measurement made using FET buffer

5.3 Analysis

The setup as described in section 5.1 was modeled using NEC (Numerical Electromagnetics Code) software to produce six predictions for currents on the wire and the received E-fields at the antenna. The models produced using NEC were,

- One wire O/C above an infinite ground plane
- One wire O/C, loaded with 50Ω on segment 1, above an infinite ground plane
- Two wire O/C Tx line
- One wire O/C above a patch ground plane
- One wire O/C above a wire-grid ground plane
- One wire, loaded with 50Ω on segment 1, above a wire-grid ground plane

The goal of this exercise was to determine which model resulted in a prediction closest to the measurements.

A comparison of the currents measured on the wire versus those predicted by NEC models demonstrates that five of the six models closely approximated the experimental data. Figure 5.2 shows a plot of the three best predictions for current. The closest approximation was predicted using the O/C wire loaded with 50Ω above an infinite ground plane, as seen in the figure 5.2 .

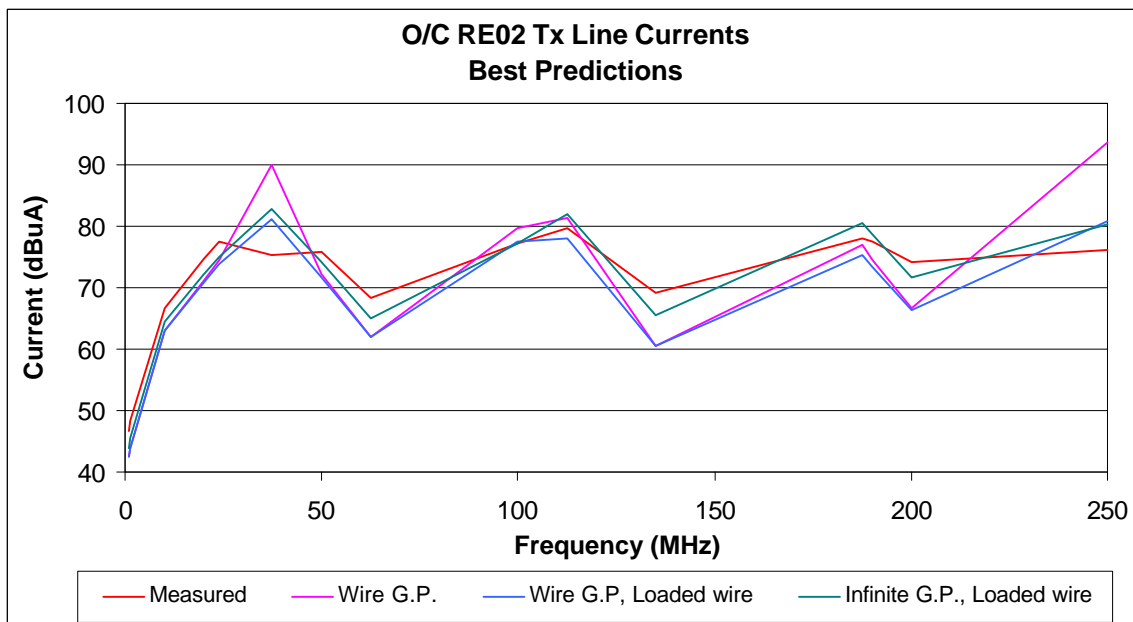


Figure 5.2 Measured current vs. three best approximations using NEC models

The worst prediction for current resulted from the model using a single surface patch ground plane, contrary to what we would expect. Upon modifying the surface patch ground plane, such that it was subdivided into multiple smaller patches, the current prediction improved significantly as shown in figure 5.3. A diagram of the new patch surface is shown in figure 5.4. The new patch surface consists of 75 patches total. The larger patches were square with sides 0.2 m long. Smaller patches were 1/2 to 1/4 of the size. The wire segment containing the voltage source terminated on the center of a 0.2m x 0.2m patch. As noted in the NEC users manual, wires must be terminated at the center of patches to produce an accurate model.

Unlike the predicted current the measured current showed peaks at 24MHz and 50MHz and the first resonance at 37.5MHz was not so obvious. The measured current was maximum at the other resonance s of 112.5MHz and 187.5MHz.

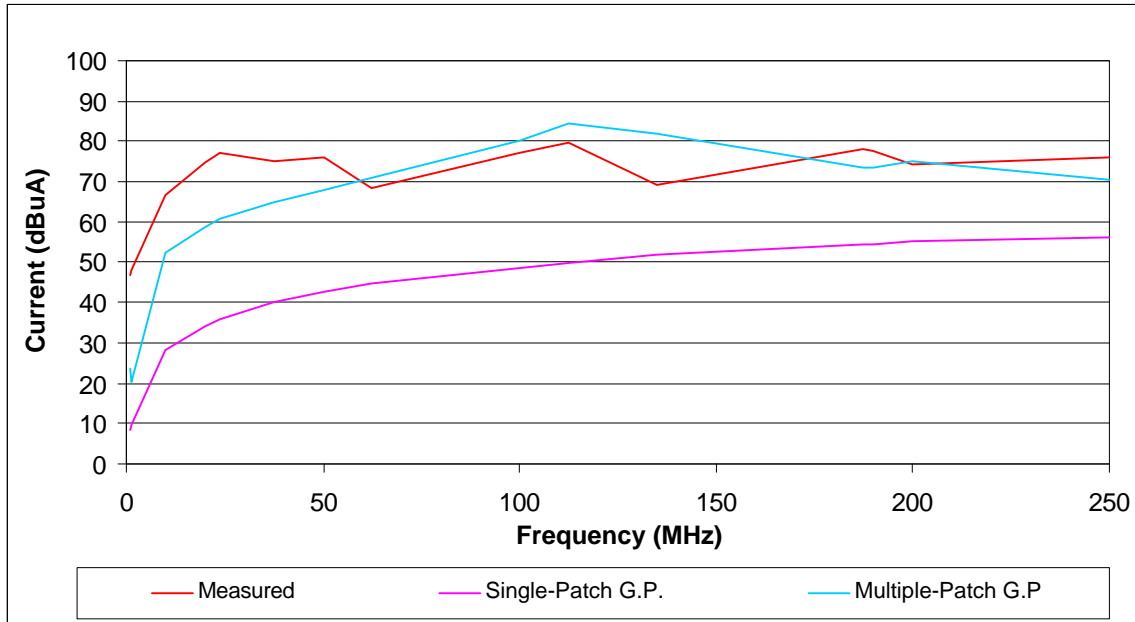


Figure 5.3 Measured current vs. single and multiple surface patch predictions. O/C line

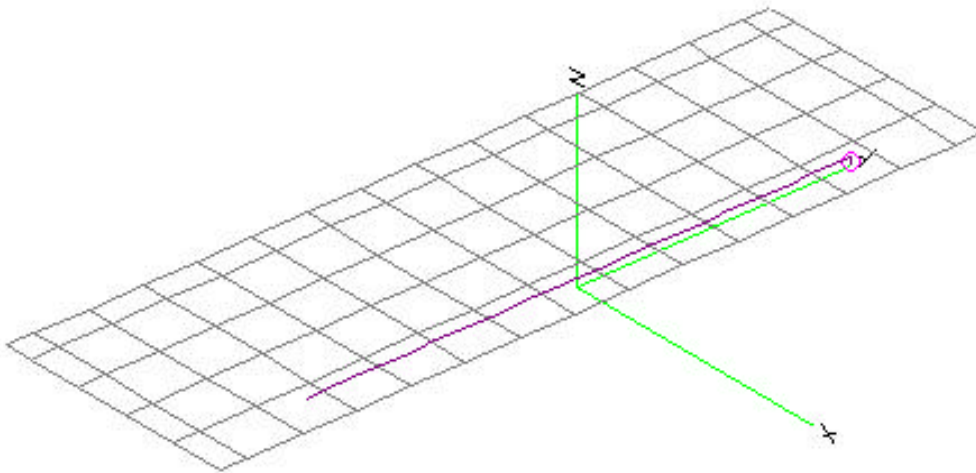


Figure 5.4 One wire O/C above a multiple surface patch ground plane

While NEC predictions for currents flowing on the wire closely approximated the actual measurements, predictions for electric field strength made by NEC did not come as close to the measured values. Figure 5.5 shows horizontal field (E_y) measurements vs. NEC predictions, and Figure 5.7 shows vertical field (E_z) measurements vs NEC predictions. Note that in these figures the predicted E-fields were not affected by adding a 50Ω load at the source on the wire, which was included in the test set up, , and thus the model with a

load on the wire over a wire-grid ground plane was omitted from the plots. As shown in the figures, E-field predictions were affected by subdividing the surface patch ground plane. The multiple-patch ground plane model made a better approximation of the measured E_y than the single-patch model. Refer to figure 5.6 for a comparison. The closest approximation to the measured E-field in the horizontal direction was made by using an equation for E_y from the transmission line theory. See appendix 1 for a description of the transmission line theory.

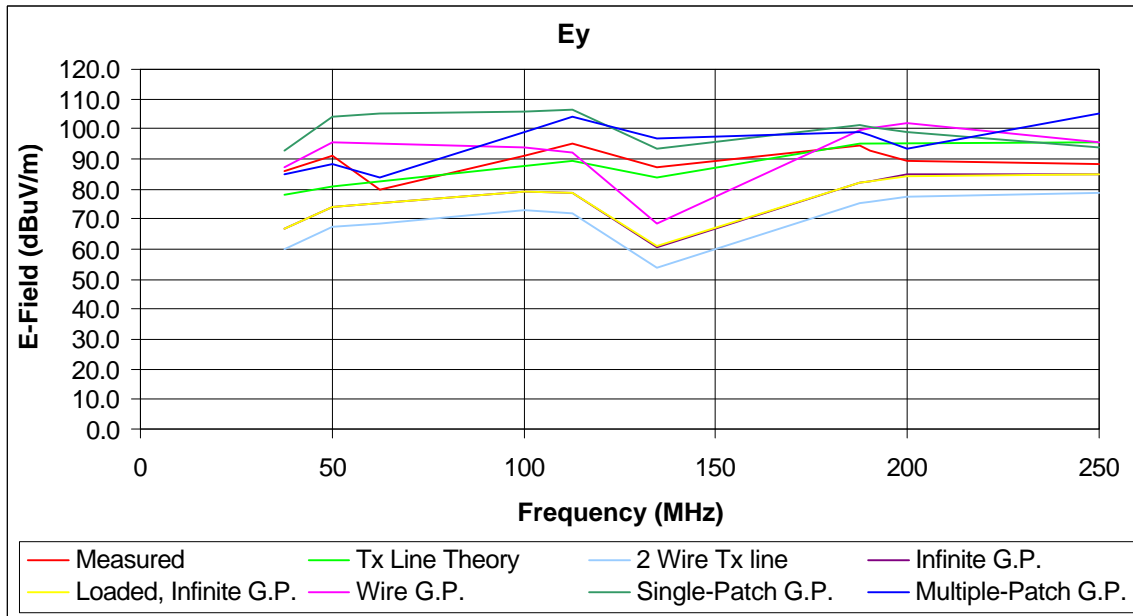


Figure 5.5 Comparison of the predicted vs the measured electric fields in the horizontal direction. O/C line

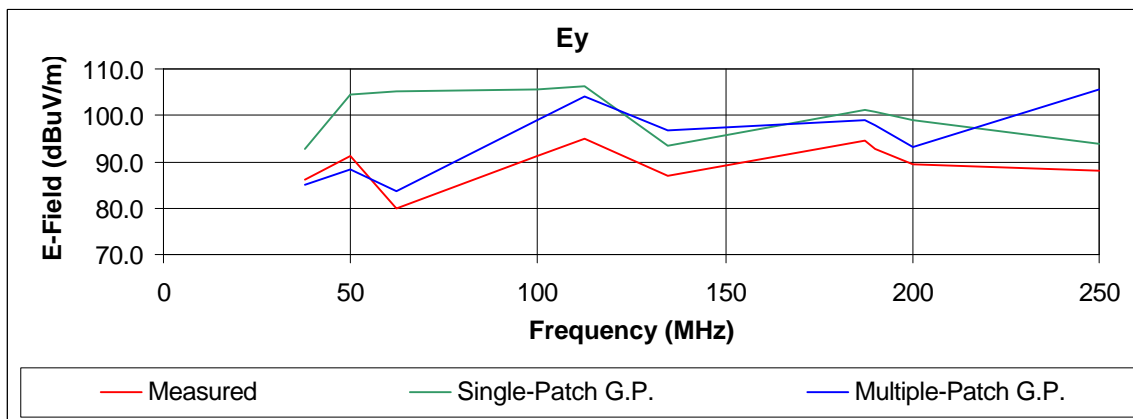


Figure 5.6 Comparison of the measured E_y vs single and multiple-patch model predictions for the O/C line.

As shown, the horizontal field predictions more closely approximate the trend developed from the measured field strength than those in the vertical direction. At 20MHz the margin of error between measured and predicted E_z values was as bad as 25.8dB and only as good as 17.5dB. For this reason, low frequency measurements were repeated using a different antenna, to determine whether or not we could trust the original measurements. Figure 5.8 shows a comparison of the original E-field measurements from 10MHz to 37.5MHz using the monopole antenna and the new measurements using the bowtie antenna. A custom calibration for the bowtie antenna was also performed at these frequencies to ensure accuracy. As shown, the new measurements are similar to the original ones.

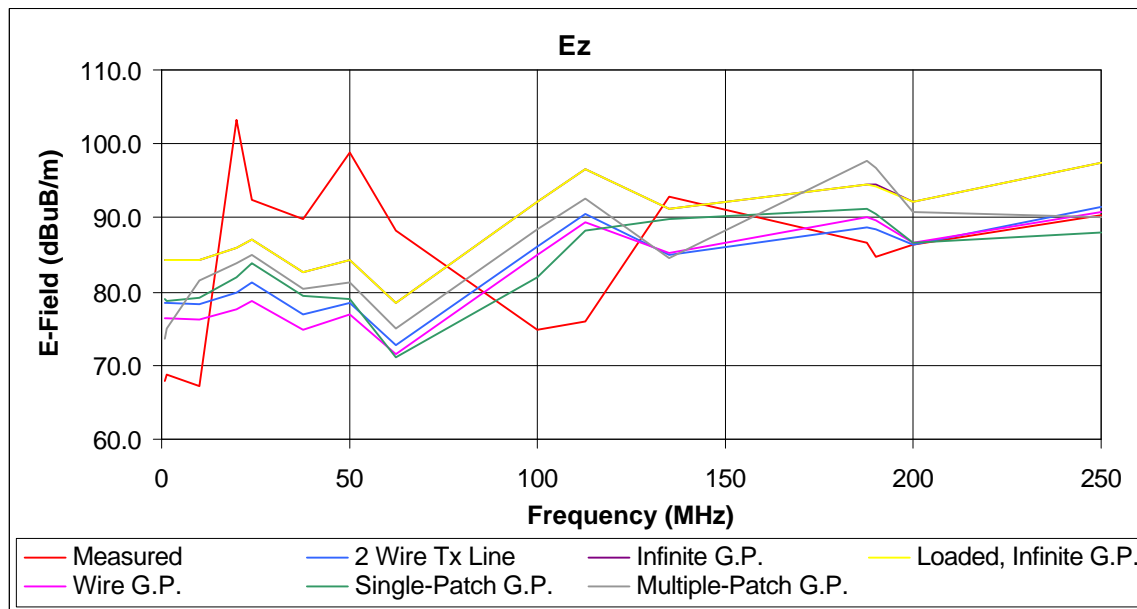


Figure 5.7 Comparison of the predicted vs the measured electric field in the vertical direction. O/C line

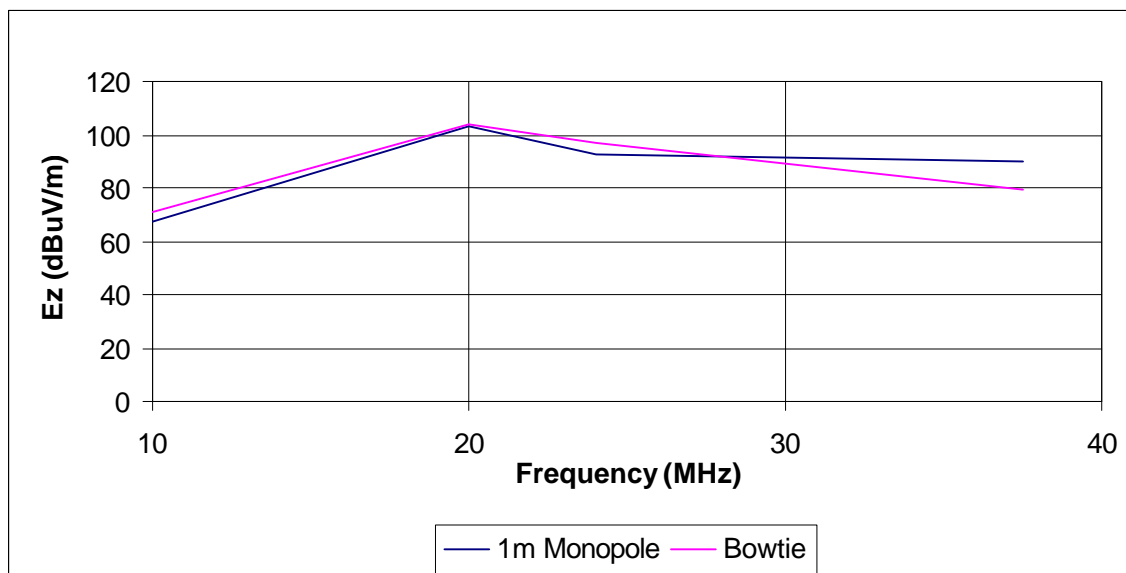


Figure 5.8 Comparison of O/C RE02 Tx line measurements taken using 1m monopole vs. bowtie antenna

To attempt an explanation of this discrepancy between measured and predicted E-fields, an equation was written to approximate the displacement currents flowing from the braid wire to the ground plane. We find fields calculated based on this model similar to those predicted by NEC, and as a result we suspected that the anomalies in the measured data could be due to resonances in the damped chamber. To test this hypothesis we moved the test setup outside and repeated the same measurements on the open area test site (OATS).

5.4 O/C Test on OATS

The test setup was identical to that inside the damped chamber/shielded room, except that the antenna was placed outside of the fiberglass hut and connected to a long microwave cable running underground to the lab. When using the monopole antenna a coupling plane could not be extended to the ground plane because of the hut wall. Electric field strengths measured were corrected by adding both antenna factors and cable attenuation. See Appendix 2 for calibration data. Tables 3 and 4 show current probe and electric field strength measurement data respectively. Figures 5.9 and 5.10, respectively, show comparisons of the horizontal and vertical e-field measurements taken on the OATS vs those taken inside the shielded room. OATS E-field measurements were normalized for equal input current to that measured in the room. Resonances and anti-resonances from the damped chamber/shielded room appear as peaks and dips on the plots of room E_y and E_z measurements. It can be seen that the first resonance resulting in the highest E field and corresponding to the highest current flow is at 37.5MHz on the OATS, as predicted, however in the chamber measurements the E field peaks at 24MHz and 50MHz and these are clearly room resonances. A bow tie antenna was used to measure the field at all locations within the room and the field did not vary significantly from close to the table,

200	72.9	9.4	1.6	83.9	76.6	9.4	1.6	87.6
250	83.2	10.5	1.9	95.6	72	10.5	1.9	84.4

* measurement made using FET buffer

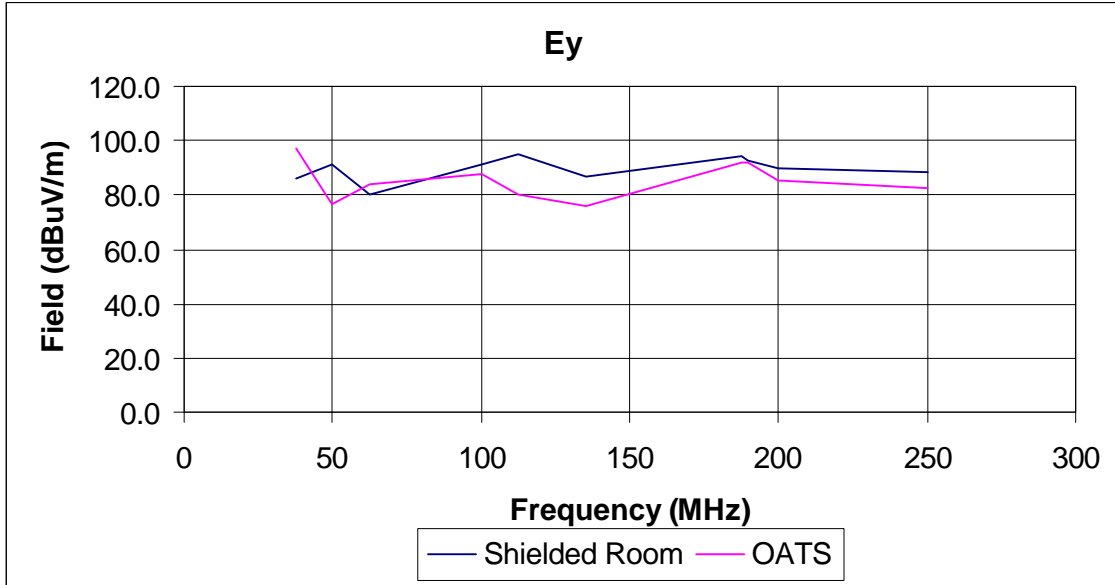


Figure 5.9 Ey measurements on OATS vs in the Shielded Room. O/C line

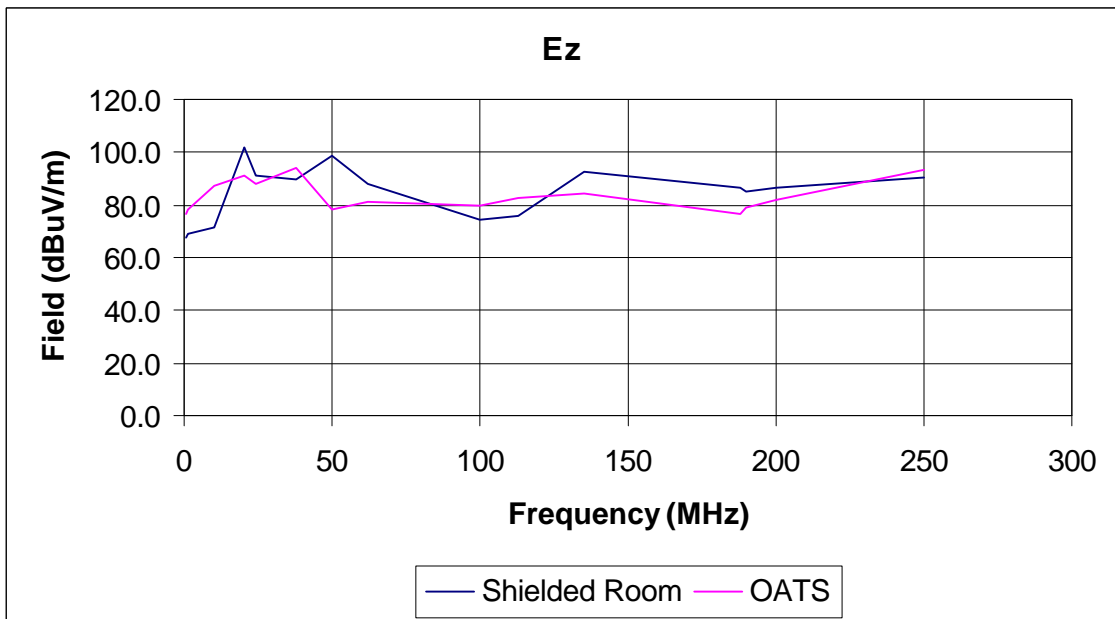


Figure 5.10 Ez measurements on OATS vs in the Shielded Room. O/C line

Comparisons of the OATS measurements with NEC predictions are shown in figures 5.11 and 5.12. In the Y direction OATS measurements lie in the middle of the differing NEC predictions with the infinite ground plane and the wire ground plane models the closest. Again the Tx line theory seems to make the most accurate prediction of the measured results in the Ey direction. Z direction E-field measurements on the OATS correlated more closely with the NEC predictions, especially at 37.5MHz, than those in the damped chamber/shielded room, however the differences in the trend still remain and may be considered too large to be useful in an EMC evaluation. The main reason for the difference is that although the current on the cable was maximum at the resonant frequencies of 37.5MHz, 112.5MHz and 187.5MHz the Ez field was maximum at only 37.5MHz and was low at 112.5MHz and 187.5MHz. The field was increasing at 250MHz and may have peaked at the 262.5MHz resonant frequency.

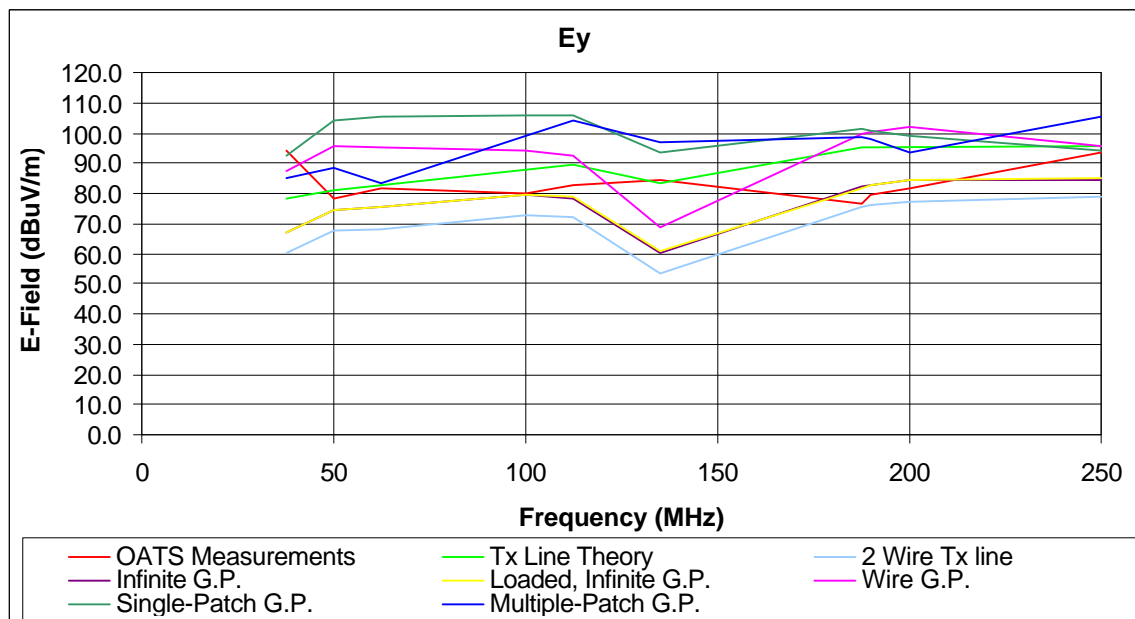


Figure 5.11 Ey measurements made on the OATS vs nec predictions. O/C line

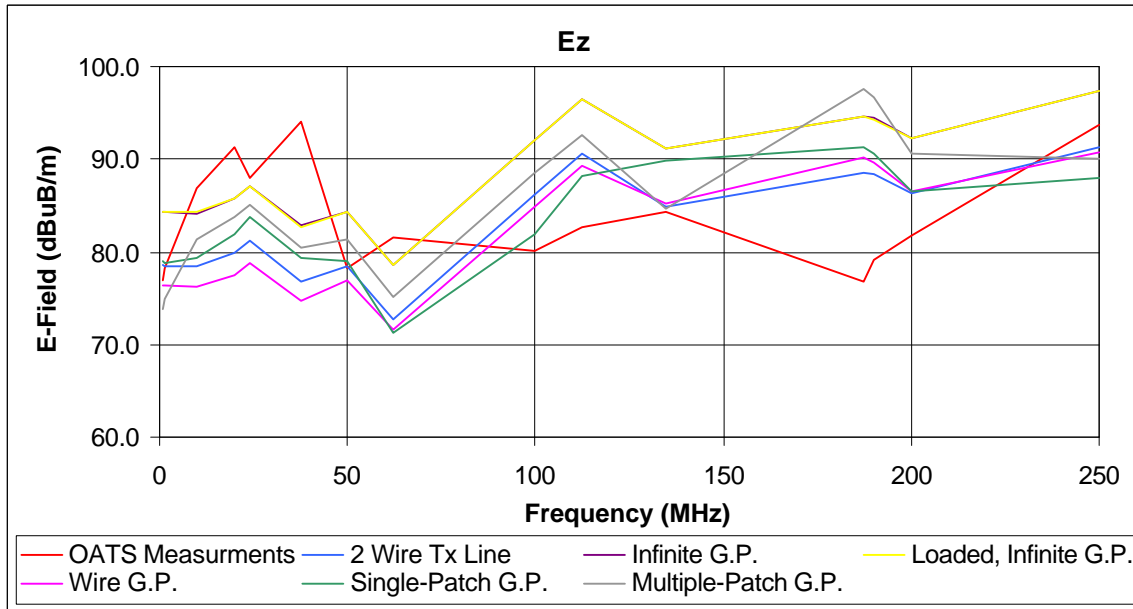


Figure 5.12 Ez measurements made on OATS vs NEC predictions. O/C line

6) Short Circuit Radiated and conducted test set up and measurements

6.1 Test Procedure

Equipment and procedure for S/C tests was identical to that for the OATS O/C test described above in sections 5.1 and 5.4 with the following exceptions. A brass plate, 10cm high and 20cm wide, was soldered to the end of the braid wire and clamped to the ground plane. This brass plate ensures a low impedance connection to the ground plane and approximates the wall of an EUT. The antennas used were again the 1m monopole for 1-24MHz, with an FET buffer for 1.0 and 1.2MHz, and a log-periodic biconical antenna for 37.5MHz to 250MHz. See figure 6.1 for a diagram of the setup. Measurements for currents and electric fields were conducted in the same fashion used in the O/C test except that the frequencies 75MHz and 150MHz were added.

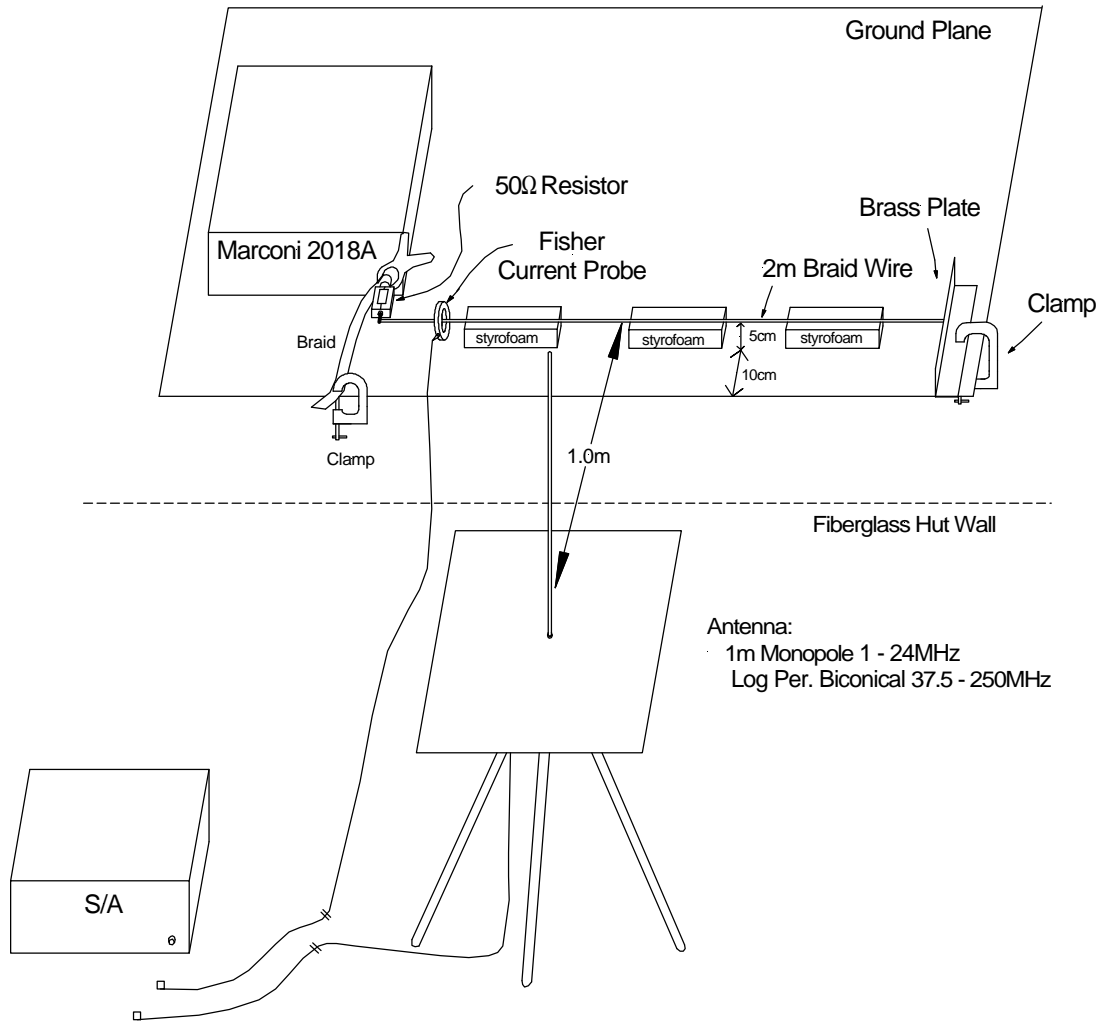


Figure 6.1 Test set up for S/C test

6.2 Test Results and Calculations

Currents and electric fields were calculated as described in section 5.2. See table 3 for Current probe measurement data and table 4 for E-field measurement data taken during the S/C test.

Table 3

Current Probe Measurement Data for S/C Test. S/C line

f (MHz)	Data (dBuV)	Current Probe Z_t (dBW)	I (dBuA)
1	89.5	6.5	83
1.2	90.1	7.2	82.9
10	92.6	14	78.6
20	87	14.6	72.4
24	84.5	14.6	69.9
37.5	52.6	15.2	37.4
50	84.1	15.5	68.6
62.3	92.3	15.2	77.1
75	84.5	15.5	69
100	66.3	14.9	51.4
112.5	91.3	15	76.3
134.9	71.5	14.8	56.7
150	67.6	14.3	53.3
187.5	82	14	68
190	83.5	13.8	69.7
200	97.6	13.3	84.3
250	96.3	11.5	84.8

Table 4
E-Field Measurement Data for S/C Test. S/C line

f (MHz)	Antenna Vertical				Antenna Horizontal			
	Data (dBuV)	AF (dB)	Cable Atten. (dB)	Total Ez (dBuV/m)	Data (dBuV)	AF (dB)	Cable Atten. (dB)	Total Ey (dBuV/m)
1	50.4	9.5	0.6	59.9				
1.2	54.1	10.6	0.6	64.7				
10	35.7	37.4	0.6	73.1				
20	52.6	28.4	0.6	81				
24	56	24.9	0.6	80.9				
37.5	49.5	20.3	0.6	69.8	60.7	20.3	0.6	81
50	50.1	17.8	0.6	67.9	68.8	17.8	0.6	86.6
62.3	78.5	14.5	0.7	93	75.1	14.5	0.7	89.6
75	82.9	9.3	0.9	92.2	59.8	9.3	0.9	69.1
100	74.1	9.7	1.2	83.8	72.6	9.7	1.2	82.3
112.5	77	10	1.2	87.0	73.5	10	1.2	83.5
134.9	74.1	12.8	1.5	86.9	74.1	12.8	1.5	86.9
150	71.3	10.7	1.5	82	66.6	10.7	1.5	77.3
187.5	72	9.4	1.6	81.4	79.5	9.4	1.6	88.9
190	67.6	9.4	1.6	77	78.2	9.4	1.6	87.6

200	79.1	9.4	1.6	88.5	76.6	9.4	1.6	86
250	75.1	10.5	1.9	85.6	72.9	10.5	1.9	83.4

6.3 Analysis

The setup as described in section 6.1 was modeled using software to produce three predictions for currents on the wire and the received E-fields at the antenna. The models produced using NEC were as follows.

- Two wire Tx line, loaded at the source end with 50Ω
- One wire TX line loaded with 50Ω at the source end and S/C at the load end, above a multiple-patch ground plane
- One wire TX line, loaded with 50Ω at the source end and S/C at the load end above a wire-grid ground plane

The infinite ground plane model was not used as explained in section 7.

Figure 6.2 shows a plot of the three predictions for current vs the measured current. The closest approximation was predicted using the wire-grid ground plane NEC model.

Figures 6.3 and 6.4 show the E_y and E_z measurements on the OATS vs nec predictions.

The Nec model using a multiple-patch ground plane makes the best prediction of both the E_y and E_z measurements for our S/C braid wire.

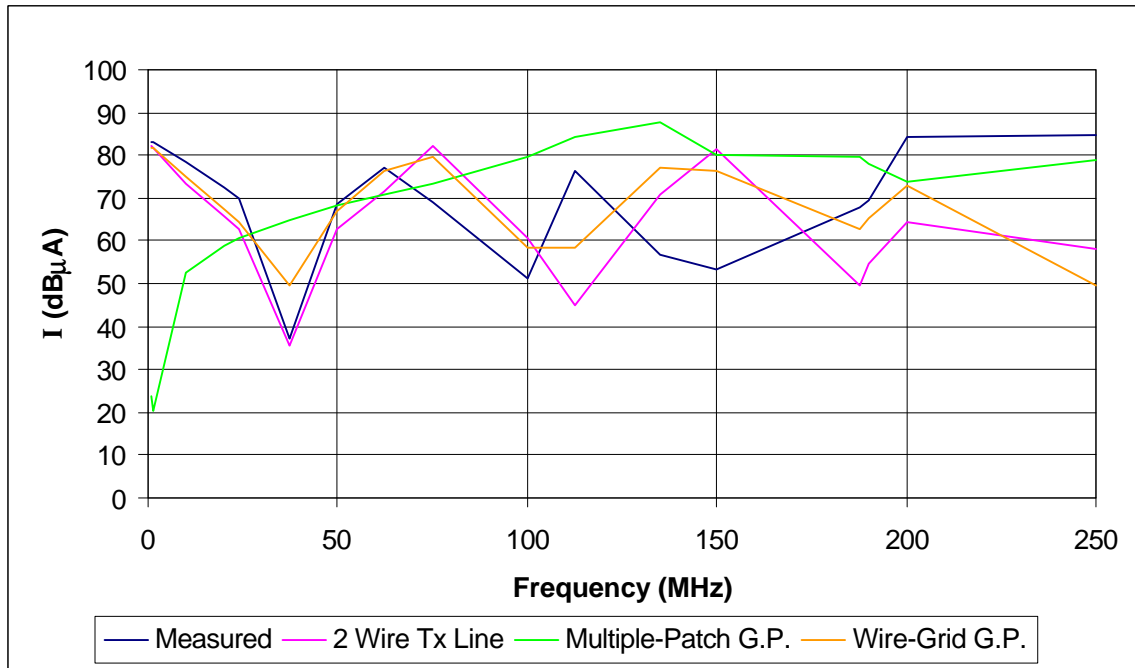


Figure 6.2 Measured current on S/C braid wire vs NEC model predictions for current

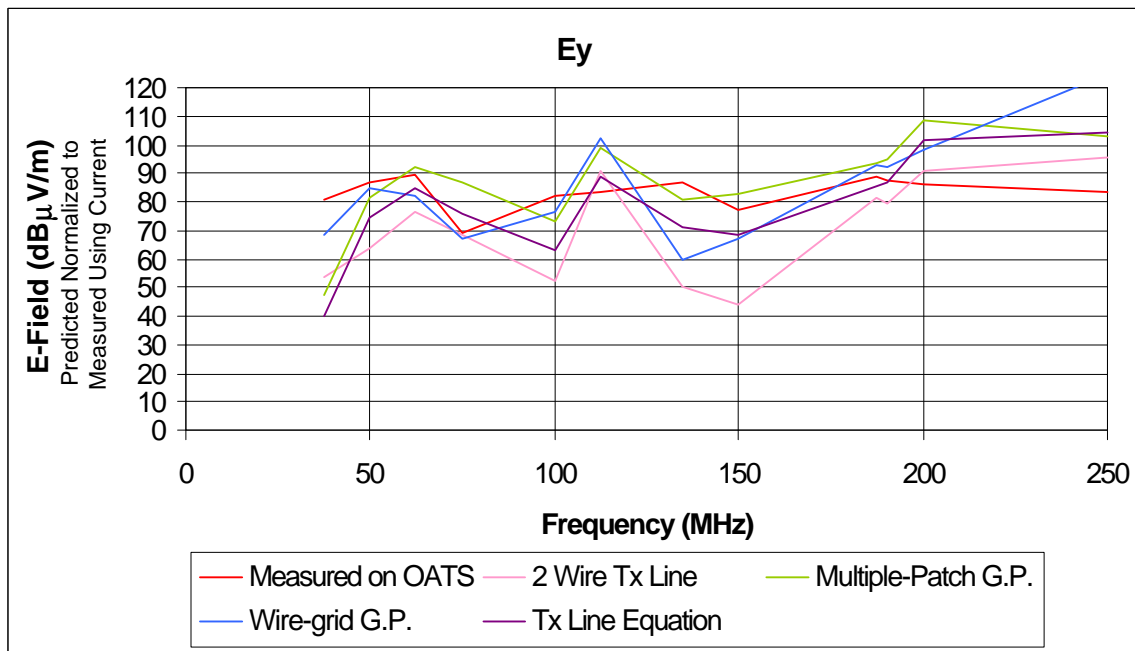


Figure 6.3 Horizontal E-field measurements vs NEC model predictions. S/C line

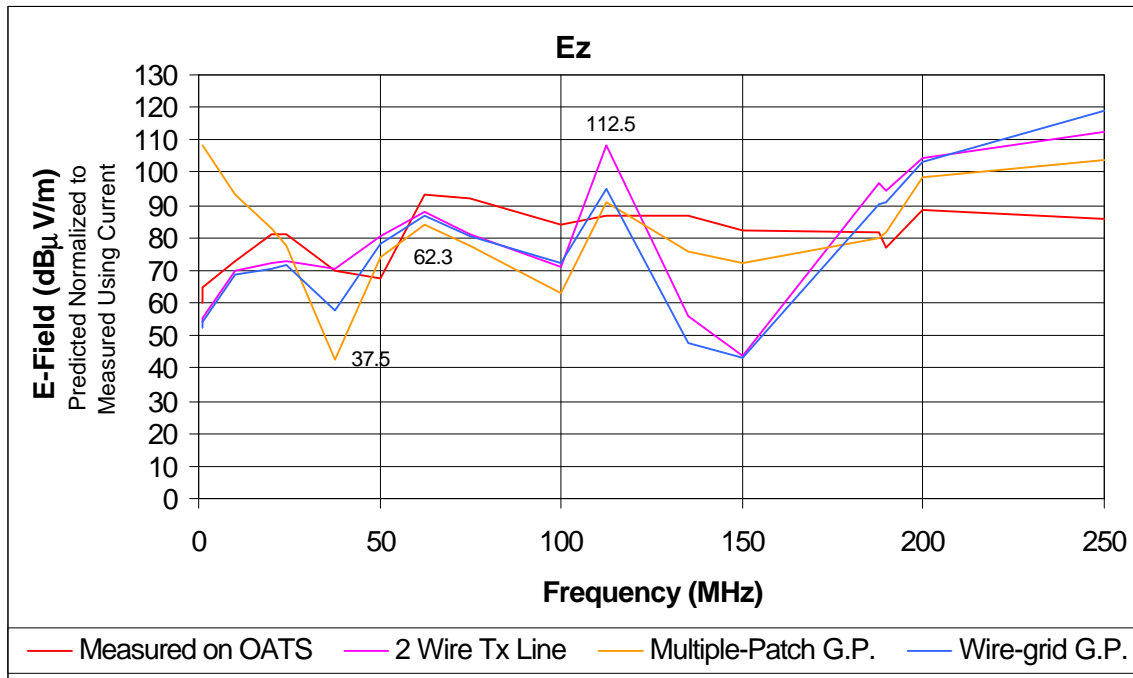


Figure 6.4 Vertical E-field measurements vs NEC model predictions. S/C line

7) NEC predicted emissions

The Numerical Electromagnetic Code used was 4nec2 version 5.3.4 authored in September 2003 by Arie. 4nec2 uses the nec-2 engine, but incorporates a user-friendly Windows interface. A copy of the software and its users manual can be obtained at the following address. <http://www.qsl.net/wb6tpu/swindex.html>

NEC allows a number of methods of modeling the ground plane under the cable and these are:

- an infinite ground plane
- a ground plane modeled as a patch
- a second wire under the wire cable, which represents the image of the wire in the ground plane
- a ground plane made up of a number of wires.

The infinite ground plane is suited to generating an electromagnetic image of the wire in the ground plane and is not suited to predicting current flow in the ground when, for example, multiple connections of wires to the ground plane are made. For this reason the infinite ground plane model is omitted from the short circuit transmission line analysis. However as it covers the electromagnetic image of the wire it should be suitable for the open circuit wire above a ground plane. To find the model which predicted emissions closest to the measured, all four configurations were tried for the open circuit prediction.

8) Conclusion

Based on comparisons between measured data and the different NEC models the correlation of the vertically polarized field may not be good enough to determine if an EUT will meet RE02/RE102 or similar radiated emission limits based on the measurement of current on the cable. For the prediction of the horizontally polarized field the simple equations introduced in reference 1 and repeated in Appendix 1 are closer to the measured data for both short circuited and open circuited lines, and this level of accuracy will typically be acceptable. The multiple patch ground plane NEC model also provides the most accurate prediction for the E_y field and may also be acceptable in predicting the E_z fields in the short circuited transmission line model.

Another large potential source of error are room resonances. Even in our well damped chamber, resonances at 24MHz and 50MHz introduce errors when comparing the room measurements to the OATS measurements. Many chambers show these TEM modes and also peaks and nulls in the field due to multiple reflections at higher frequencies, which are not predominant in our damped chamber/shielded room.

A simple equation was developed and used to predict the vertically polarized field radiated from the line at 1.0MHz and 1.2MHz. We will try to develop this equation to include long line effects and if successful this will be included as an update to this report. This report again validates the simple TX line equation based on radiation resistance and radiated power, by measurements, presented in reference 1 and reproduced in Appendix 1 of this report.

Appendix 1

Emission from Transmission-Line Geometries (Taken from Reference 1)

To calculate the radiation from a transmission line made up of either two cables or a cable above a ground plane, use is made of the concept of the radiation resistance of the line. Radiation resistance of an antenna or transmission line is used to describe that part of the conductor resistance that converts a fraction of the power delivered to the load into radiated power. In an efficient antenna, the radiation resistance is designed to be high and the resistance, which converts the input power into heat, is low. In the transmission line, the opposite is true. The radiation resistance for a resonant section of two-wire line length or $\lambda/2$ (or integral multiples of $\lambda/2$ when the line is short-circuited (symmetrical connection), or $\lambda/4$ and other multiples when the line is open circuited as in:

$$l = \frac{(2k + 1) \lambda}{4}$$

where $k = 0, 1, 2, 3, \dots$

when the line is open-circuited or terminated in a load higher than Z_c (asymmetrical connection) or short circuited at both ends (symmetrical connection) then the radiation resistance is,

$$30\beta^2 b^2$$

where b is either the distance between the two-conductor line or twice the height of the cable above a ground plane. The radiated power for the resonant line is given by

$$30\beta^2 b^2 I^2$$

where I is the current flow on the line, either measured or calculated. For the majority of EMI conditions, the radiated noise covers a wide range of frequencies, and resonant line conditions can be expected. For example, when the source of current is converter or digital logic noise, the harmonics may range from kilohertz up to 500MHz.

The magnetic field some distance R from the line is

$$H = \sqrt{\frac{Pk}{4\pi R^2 Z_w}}$$

where

P = radiated power
 Z_w = wave impedance

k = directivity, which is approximately 1.5 for a current loop resonant line and 1.0 for a nonresonant line
 R = distance in meters

and the electric field is

$$E = \sqrt{\frac{Z_w P k}{4\pi R^2}}$$

In the near field, the wave impedance is close to the characteristic impedance Z_c of the transmission line, which may be calculated from

$$Z_c = \sqrt{\frac{(Z_i + j\omega l_e)\omega l_e}{jk^2}}$$

where

Z_i = distributed series resistance of the two wire line [Ω/m]

$$k = \omega \sqrt{\mu_0 \epsilon_0} = \frac{2\pi}{\lambda}$$

$$l_e = \frac{\mu_0}{\pi} \ln \frac{2h}{a}$$

$$\mu_0 = 4\pi \times 10^{-7} \text{ [H/m]}$$

a = diameter of wire [m]

The wave impedance then changes linearly until the near-field/far-field interface, at which $Z_w = 377\Omega$. The E field radiated by the current loop may be obtained from $E = H \times Z_w$. The equation for calculating the wave impedance in the near field is

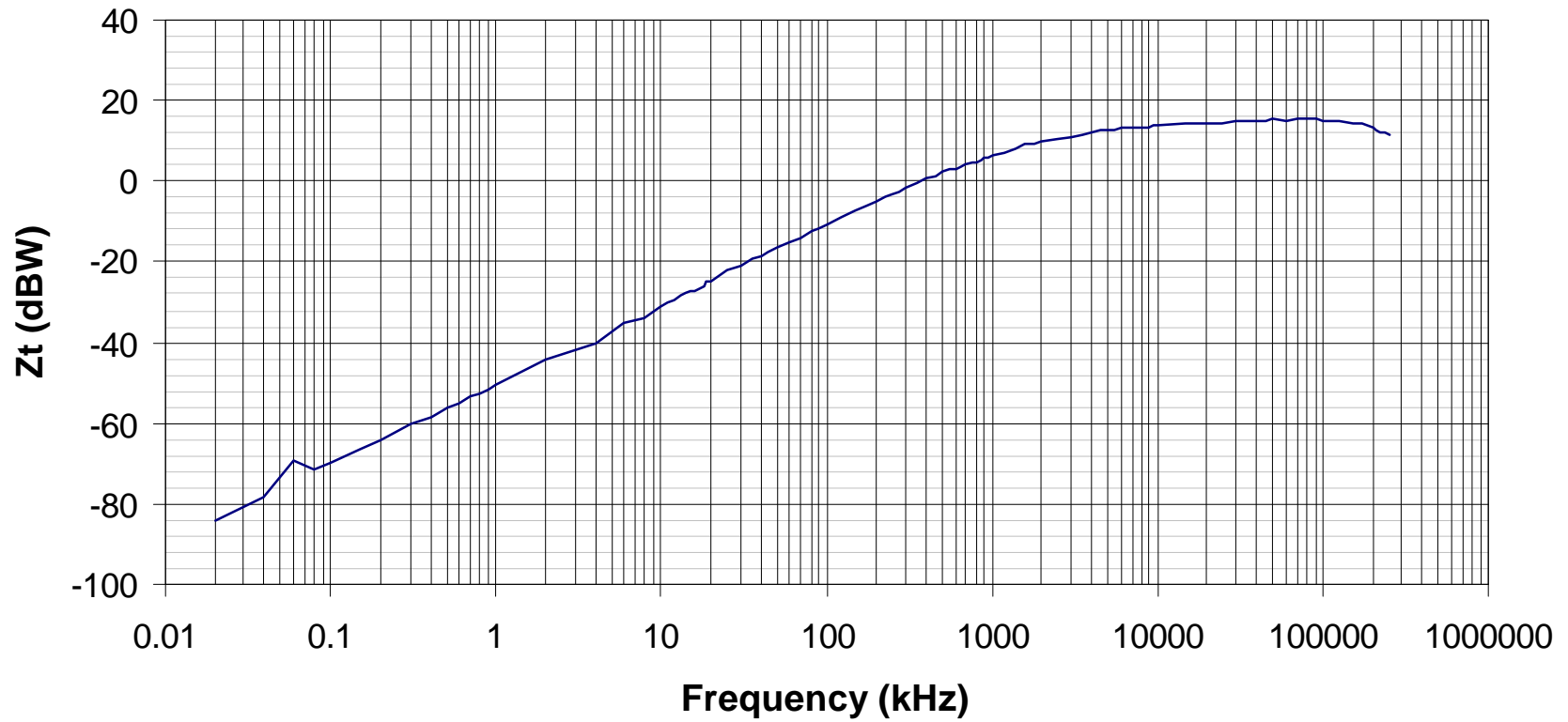
$$Z_w = \frac{\lambda/2\pi - R}{\lambda/2\pi} (Z_c - 377) + 377 \quad (Z_w < 377 \Omega)$$

where R is the distance from the radiation source, in meters.

Frequency (kHz)	Z _t (dBΩ)
90	-11.6
100	-10.7
125	-8.8
150	-7.2
175	-6.0
200	-5.0
225	-4.1
250	-3.5
275	-2.5
300	-1.6
350	-0.3
400	0.6
450	1.5
500	2.2
550	2.8
600	3.1
650	3.7
700	4.0
750	4.7
800	5.0
850	5.3
900	5.6
950	5.9
1000	6.5
1200	7.2
1400	8.1
1600	9.0
1800	9.3
2000	10.0
2500	10.6
3000	11.2
3500	11.8
4000	12.1
4500	12.5
5000	12.8
5500	12.8
6000	13.1
6500	13.1
7000	13.1
7500	13.4
8000	13.4
8500	13.4

Frequency (kHz)	Z_t (dBΩ)
9000	13.4
9500	14.0
10000	14.0
15000	14.3
20000	14.6
25000	14.6
30000	14.9
35000	15.2
40000	15.2
45000	15.2
50000	15.5
60000	15.2
70000	15.3
80000	15.6
90000	15.3
100000	14.9
125000	15.2
150000	14.3
175000	14.6
200000	13.3
210000	12.4
225000	12.0
235000	12.1
250000	11.5

Fisher Model No. F-33-1 S/N 115 Current Probe Calibration
Mar 8, 2004



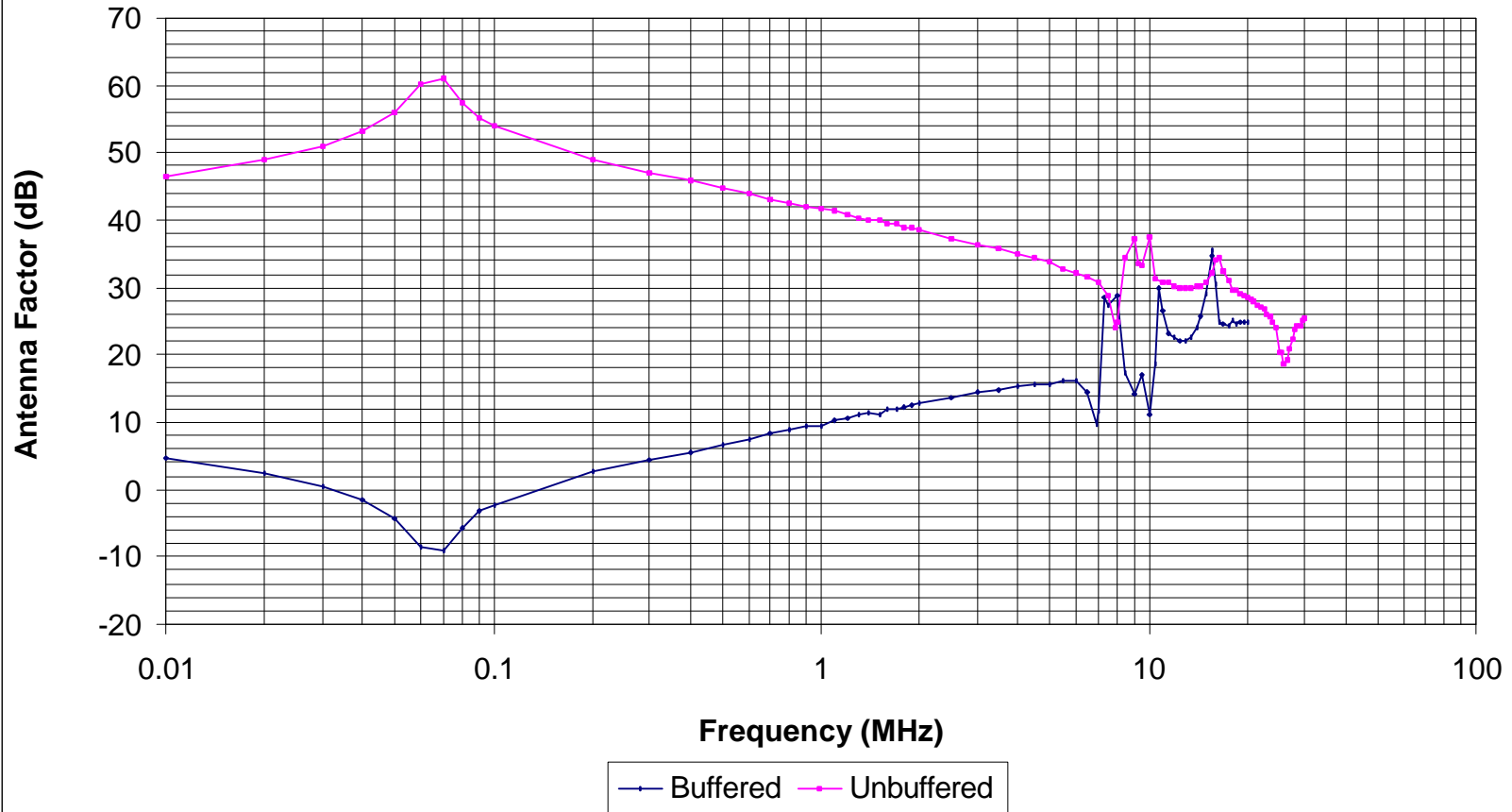
9.0	8.44E-05	37.3
9.25	2.08E-04	33.5
9.5	2.19E-04	33.4
10.0	9.16E-05	37.4
10.5	3.78E-04	31.4
11.0	4.66E-04	30.7
11.5	4.87E-04	30.7
12.0	5.64E-04	30.3
12.5	6.22E-04	30.0
13.0	6.70E-04	29.9
13.5	6.95E-04	29.9
14.0	6.89E-04	30.1
14.5	6.73E-04	30.3
15.0	6.21E-04	30.8
15.5	4.76E-04	32.1
16.0	3.17E-04	34.0
16.5	3.02E-04	34.4
17.0	5.04E-04	32.3
17.5	6.73E-04	31.1
18.0	9.60E-04	29.7
18.5	1.01E-03	29.6
19.0	1.15E-03	29.2
19.5	1.28E-03	28.8
20.0	1.44E-03	28.4
20.5	1.54E-03	28.2
21.0	1.69E-03	27.9
21.5	1.90E-03	27.5
22.0	2.16E-03	27.1
22.5	2.42E-03	26.7
23.0	2.81E-03	26.1
23.5	3.26E-03	25.6
24.0	3.86E-03	24.9
24.5	5.02E-03	23.9
25.0	1.12E-02	20.5
25.5	1.14E-02	20.5
26.0	1.73E-02	18.8
26.5	1.60E-02	19.2
27.0	1.10E-02	20.9
27.5	7.97E-03	22.4
28.0	6.15E-03	23.6
28.5	5.27E-03	24.3
29.0	5.36E-03	24.3
29.5	4.48E-03	25.2
30.0	4.26E-03	25.5

1m Monopole Calibration at 1m in the Shielded Room
Uncoupled, With FET Buffer
August 8, 2003

Frequency (MHz)	Antenna Factor (dB)
0.01	4.7
0.02	2.3
0.03	0.4
0.04	-1.4
0.05	-4.3
0.06	-8.5
0.07	-9.2
0.08	-5.7
0.09	-3.3
0.1	-2.2
0.2	2.8
0.3	4.5
0.4	5.6
0.5	6.7
0.6	7.6
0.7	8.3
0.8	8.9
0.9	9.4
1.0	9.5
1.1	10.2
1.2	10.6
1.3	11.1
1.4	11.4
1.5	11.2
1.6	11.9
1.7	11.9
1.8	12.2
1.9	12.4
2.0	12.7
2.5	13.6
3.0	14.5
3.5	14.8
4.0	15.2
4.5	15.5
5.0	15.7
5.5	16.1
6.0	16.1
6.5	14.6
6.91	9.6
7.0	11.6
7.34	28.6
7.5	27.5
8.0	28.7

8.5	17.4
9.0	14.2
9.5	16.9
10.0	11.0
10.5	18.8
10.8	29.9
11.0	26.5
11.5	23.2
12.0	22.5
12.5	22.0
13.0	22.1
13.5	22.6
14.0	23.9
14.5	25.8
15.0	29.1
15.5	34.6
15.7	26.6
16.0	30.6
16.5	24.9
17.0	24.5
17.5	24.4
18.0	25.2
18.5	24.6
19.0	24.8
19.5	24.8
20.0	24.9

1m Monopole Calibration at 1m in the Shielded Room
Uncoupled With and Without FET Buffer
August 8, 2003



1m Monopole Calibration at 1m in the Shielded Room
 Coupled, Without FET Buffer
 August 8, 2003

Frequency (MHz)	Gain (num)	Antenna Factor (dB)
0.01	6.12E-08	39.1
0.02	5.93E-08	42.3
0.03	6.01E-08	44.0
0.04	5.81E-08	45.4
0.05	5.63E-08	46.5
0.06	5.43E-08	47.4
0.07	4.92E-08	48.5
0.08	4.52E-08	49.5
0.09	3.68E-08	50.9
0.1	3.33E-08	51.8
0.134	2.69E-08	54.0
0.2	7.90E-08	51.0
0.3	2.18E-08	48.4
0.4	4.21E-07	46.8
0.5	6.54E-07	45.8
0.6	9.66E-07	44.9
0.7	1.31E-06	44.3
0.8	1.72E-06	43.7
0.9	2.17E-06	43.2
1.0	2.67E-06	42.7
1.1	3.30E-06	42.2
1.2	3.99E-06	41.8
1.3	4.63E-06	41.5
1.4	5.60E-06	41.0
1.5	5.93E-06	41.0
1.6	6.47E-06	40.9
1.7	7.28E-06	40.7
1.8	8.26E-06	40.4
1.9	9.45E-06	40.0
2.0	1.07E-05	39.7
2.5	1.66E-05	38.8
3.0	2.51E-05	37.8
3.5	3.40E-05	37.1
4.0	4.46E-05	36.5
4.5	5.50E-05	36.1
5.0	6.47E-05	35.9
5.5	7.54E-05	35.6
6.0	8.61E-05	35.4
6.5	9.33E-05	35.4
7.0	9.70E-05	35.6
7.5	9.48E-05	36.0
8.0	8.91E-05	36.5

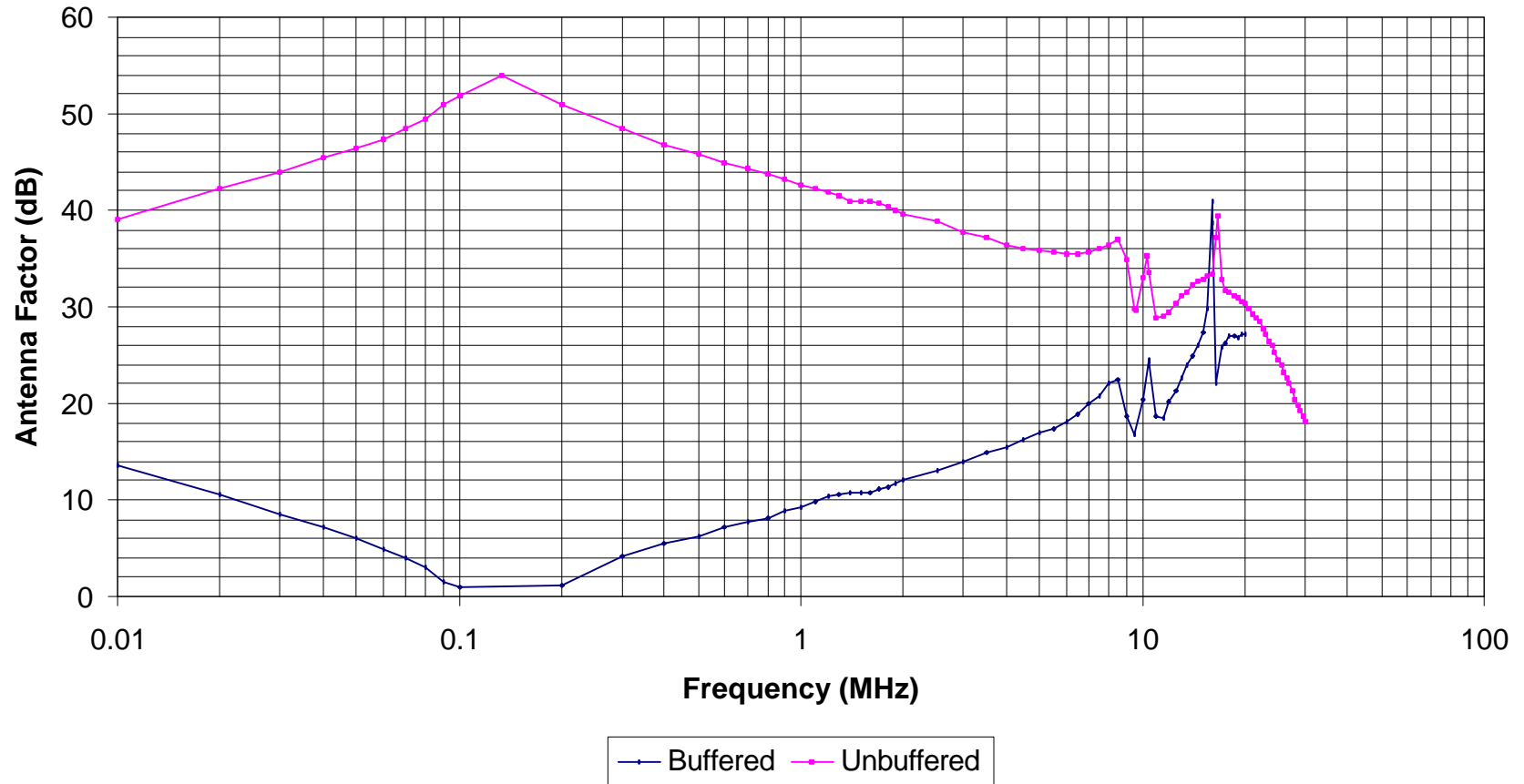
8.5	8.74E-05	36.9
9.0	1.45E-04	34.9
9.5	4.84E-04	29.9
9.59	5.23E-04	29.6
10.0	2.49E-04	33.0
10.31	1.53E-04	35.3
10.5	2.28E-04	33.6
11.0	7.30E-04	28.8
11.5	7.20E-04	29.0
12.0	6.70E-04	29.5
12.5	5.74E-04	30.4
13.0	5.08E-04	31.1
13.5	4.70E-04	31.6
14.0	4.15E-04	32.3
14.5	3.92E-04	32.7
15.0	3.87E-03	32.9
15.5	3.69E-04	33.2
16.0	3.64E-04	33.4
16.5	1.56E-04	37.2
16.6	9.59E-04	39.4
17.0	4.39E-04	32.9
17.5	5.89E-04	31.7
18.0	6.41E-04	31.5
18.5	7.06E-04	31.2
19.0	7.68E-04	30.9
19.5	8.55E-04	30.6
20.0	9.29E-04	30.3
20.5	1.08E-03	29.8
21.0	1.23E-03	29.3
21.5	1.43E-03	28.8
22.0	1.60E-03	28.4
22.5	1.88E-03	27.8
23.0	2.26E-03	27.1
23.5	2.62E-03	26.5
24.0	3.00E-03	26.0
24.5	3.64E-03	25.3
25.0	4.41E-03	24.5
25.5	5.17E-03	23.9
26.0	6.05E-03	23.3
26.5	7.25E-03	22.6
27.0	8.57E-03	22.0
27.5	1.03E-02	21.3
28.0	1.27E-02	20.4
28.5	1.48E-02	19.8
29.0	1.72E-02	19.3
29.5	2.03E-02	18.6
30.0	2.29E-02	18.2

1m Monopole Calibration at 1m in the Shielded Room
Coupled, With FET Buffer
August 8, 2003

Frequency (MHz)	Antenna Factor (dB)
0.01	13.5
0.02	10.5
0.03	8.5
0.04	7.1
0.05	6.0
0.06	5.0
0.07	3.9
0.08	3.0
0.09	1.6
0.1	1.0
0.2	1.1
0.3	4.1
0.4	5.4
0.5	6.2
0.6	7.1
0.7	7.8
0.8	8.1
0.9	8.9
1.0	9.3
1.1	9.8
1.2	10.3
1.3	10.6
1.4	10.8
1.5	10.7
1.6	10.8
1.7	11.1
1.8	11.4
1.9	11.7
2.0	12.0
2.5	13.0
3.0	14.0
3.5	14.9
4.0	15.5
4.5	16.2
5.0	16.9
5.5	17.4
6.0	18.2
6.5	18.8
7.0	20.0
7.5	20.8
8.0	22.1
8.5	22.4

9.0	18.7
9.5	16.8
10.0	20.3
10.41	24.5
10.5	24.4
11.0	18.7
11.5	18.4
12.0	20.1
12.5	21.4
13.0	22.6
13.5	24.0
14.0	24.9
14.5	26.0
15.0	27.4
15.5	29.8
15.95	41.0
16.0	38.7
16.5	22.1
17.0	25.8
17.5	26.3
18.0	26.9
18.5	26.9
19.0	26.8
19.5	27.2
20.0	27.1

**1 m Monopole Calibration at 1m in the Shielded Room
Coupled With and Without FET Buffer
August 8, 2003**



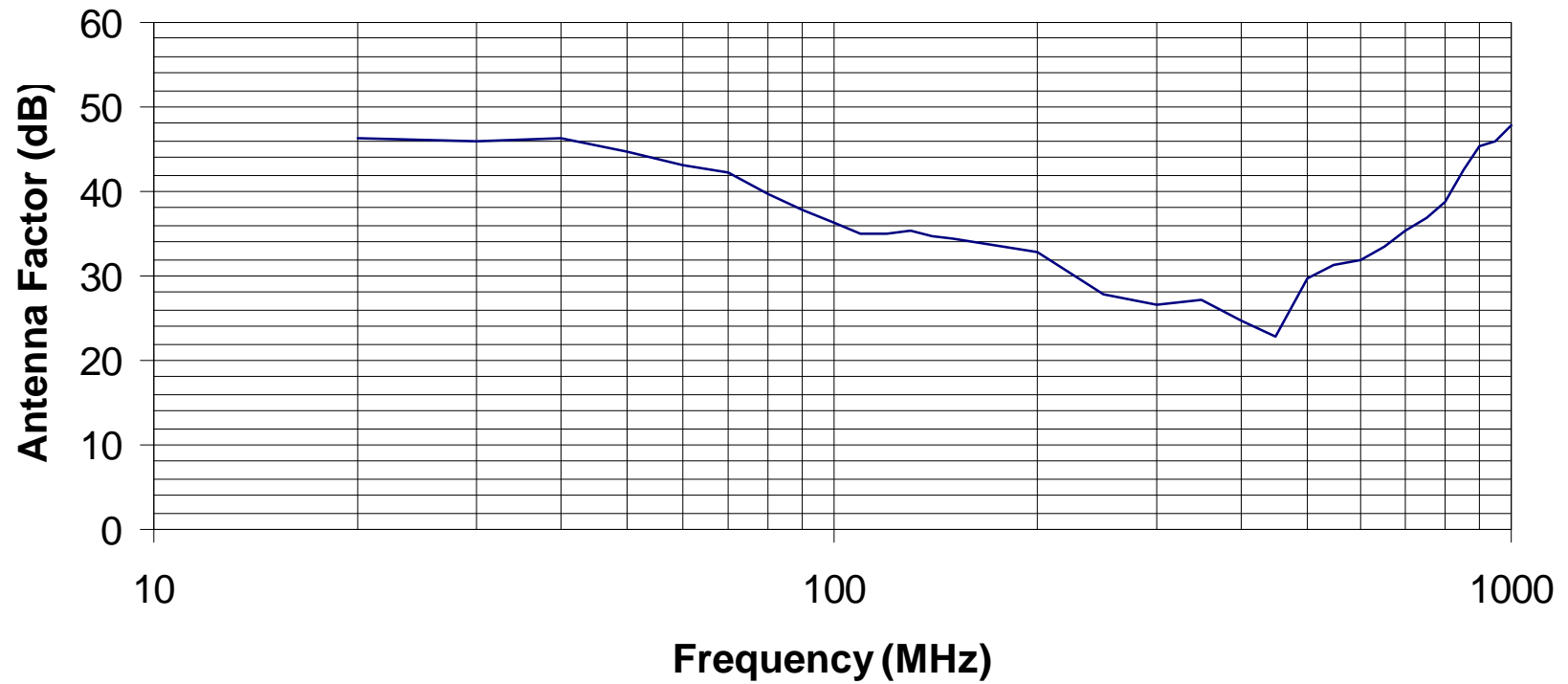
250.5	5.8211	10.5
252.5	5.6555	10.7
260.5	5.835	10.9
270.5	5.0575	11.8
271.5	4.8982	12
275.5	4.4607	12.5
280.5	3.9285	13.2
282.5	3.5508	13.7
285.5	2.8868	14.7
288.5	2.7162	15.1
290.5	2.8345	15
291.5	3.0582	14.7
293.5	3.4312	14.2
295.6	3.9939	13.6
297.6	3.8756	13.8
299.6	4.1952	13.5
300.6	4.5258	13.2
305.6	5.1272	12.8
310.6	5.8069	12.4
311.6	6.0442	12.3
323.6	6.2702	12.4
325.6	6.3091	12.5
330.6	5.9648	12.9
335.6	4.8711	13.9
339.6	3.9699	14.9
340.6	4.2812	14.6
345.7	4.6656	14.3
349.7	5.0806	14
350.7	5.2802	13.9
353.7	5.519	13.8
355.7	5.7586	13.6
357.7	5.5816	13.8
360.7	5.0511	14.3
368.7	5.7536	14
372.7	5.6122	14.2
375.7	5.2616	14.5
380.7	4.6171	15.2
387.7	3.3986	16.7
390.7	4.0988	15.9
392.7	4.5907	15.5
394.7	5.3344	14.9
400.8	6.2539	14.3
405.8	7.0558	13.9

410.8	6.8925	14.1
420.8	6.5742	14.5
430.8	5.6113	15.4
440.8	5.3401	15.8
450.9	4.9069	16.4
460.9	4.5015	17
470.9	4.433	17.2
471.9	4.7766	16.9
475.9	4.8172	16.9
480.9	4.5273	17.3
485.9	4.1053	17.8
490.9	4.1476	17.9
500.0	4.2238	17.9
509.0	4.4562	17.9
510.0	4.6272	17.7
520.0	4.7019	17.8
526.7	4.9415	17.7
532.5	4.1696	18.5
536.4	2.6255	20.6
537.3	2.1953	21.4
538.3	1.7071	22.5
539.2	1.3774	23.5
540.2	1.0711	24.6
541.2	1.2856	23.8
542.1	1.6591	22.7
545.0	2.4784	21
550.8	2.4168	21.2
555.6	1.7621	22.7
556.6	1.5841	23.1
560.4	1.3313	23.9
561.4	1.4339	23.6
565.2	1.6691	23
566.2	1.7327	22.9
567.1	1.8662	22.6
568.1	1.9373	22.4
569.1	2.0865	22.1
570.0	2.2473	21.8
575.8	2.921	20.8
580.6	3.5289	20
585.4	3.9649	19.6
590.2	4.1427	19.5
595.0	3.748	20
600.8	3.2734	20.6

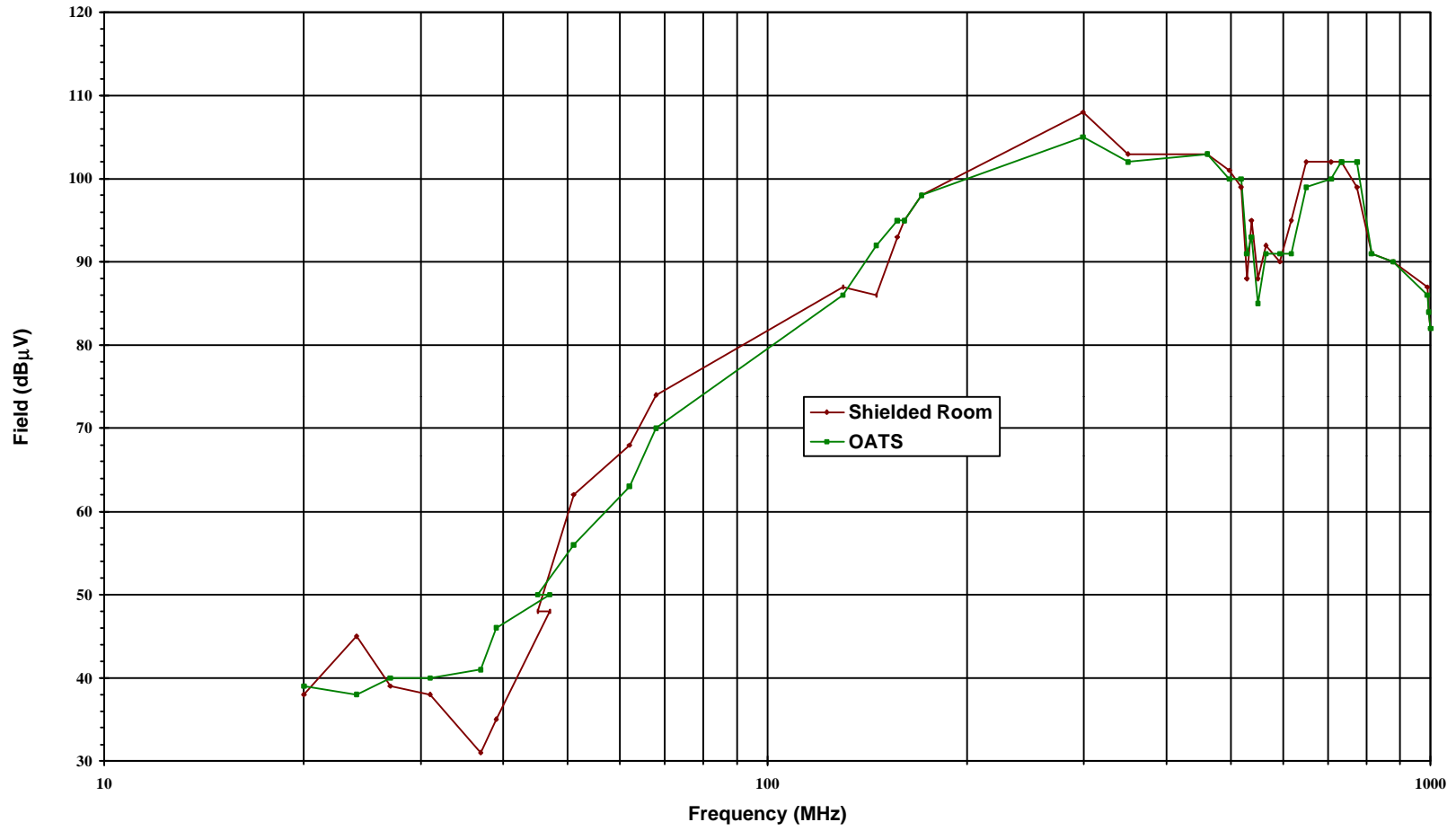
604.6	3.5422	20.4
605.6	3.6767	20.2
610.4	3.7102	20.2
612.3	3.7219	20.3
615.2	3.7394	20.3
618.1	3.7526	20.3
619.1	3.4995	20.6
621.0	3.5104	20.6
623.9	3.3992	20.8
624.8	3.1699	21.1
628.7	3.1894	21.2
630.6	3.0834	21.3
632.5	3.3255	21
635.4	3.592	20.7
637.4	4.0146	20.3
638.3	3.8753	20.4
639.3	4.3297	20
640.2	4.6624	19.7
644.1	5.2205	19.2
645.1	5.6281	18.9
648.9	6.0805	18.6
650.8	6.7956	18.2
656.6	6.8638	18.2
660.4	6.896	18.2
662.4	6.9241	18.2
663.3	6.9262	18.2
664.3	7.458	17.9
665.3	7.2069	18.1
667.2	6.9664	18.3
671.0	7.0065	18.3
672.0	7.2715	18.2
678.7	7.0869	18.3
680.6	7.107	18.4
683.5	7.1371	18.4
690.3	7.2074	18.4
700.8	7.3179	18.5
705.7	6.8526	18.8
710.5	6.4166	19.2
720.1	5.8364	19.7
730.7	6.5991	19.3
740.3	6.9369	19.2
750.9	7.036	19.3
759.5	6.8676	19.5

760.5	6.6276	19.6
769.1	6.468	19.8
770.1	6.249	20
780.7	6.8036	19.7
788.4	6.8707	19.8
789.3	6.6379	19.9
790.3	6.646	20
795.1	6.9373	19.8
800.9	6.735	20
810.5	6.8158	20.1
820.1	6.4142	20.4
824.9	6.6863	20.3
830.7	6.0424	20.8
837.4	5.6718	21.1
843.2	5.3113	21.5
850.9	4.8045	22
853.8	4.6517	22.2
861.5	4.6937	22.2
862.4	4.5342	22.4
865.3	4.3848	22.5
870.1	4.7408	22.3
900.0	5.0873	22.2
909.6	5.7294	21.8
945.2	5.9536	22
950.9	5.5708	22.3
960.6	4.6967	23.2
970.2	4.1079	23.8
971.1	3.9632	24
976.9	3.4524	24.6
980.8	3.1105	25.1
985.6	2.8051	25.6
996.2	2.5444	26.1
1000.0	2.3756	26.5

Bowtie Free Space Calibration 1.2m
Calibrated April 7, 2003 - Bowtie3.cal



Shielded Room / OATS Correlation



Reference 1 Electromagnetic Compatibility Principles and Applications. Marcel Dekker
2001. David A. Weston.